International Journal of Applied Mathematics

Volume 38 No. 7s, 2025

ISSN: 1311-1728 (printed version); ISSN: 1314-8060 (on-line version)

PREPARATION AND FABRICATION OF A GAS SENSORCR$_2$O$_3$ IMPREGNATED WITH RARE EARTH ELEMENTS (AU) AND PRECIPITATED BY CHEMICAL BATH TECHNIQUE

Haider Mahmood Abdul Majeed[1], Niran Fadhel Abd Al Jabbar[2]

[1,2]Tikrit University / College of Education for Pure Sciences / Department of Physics

Email: haedar_mahmood@st.tu.edu.iq , niran.fadhil64@tu.edu.iq .

Abstract

Thin films were prepared from Cr_2O_3 doped with gold (2–8%) using the chemical bath technique, and their structural, optical, electrical, and photosensitive properties were studied. XRD results showed that the primary phase was rhombohedral Cr_2O_3, with Au peaks appearing at higher percentages. The crystallite size gradually decreased with doping due to the increased growth centers. SEM images showed that the grain size decreased from ~85 nm at 2% to ~53 nm at 8%, with a rougher surface rich in active sites. Optically, the absorbance increased and the transmittance decreased with increasing Au percentage, with the energy gap narrowing from ~3.05 eV to ~2.72 eV due to plasmonic resonance and electronic structure modification. Electrically, Hall measurements confirmed that all films were p-type, and that the carrier concentration and mobility increased with doping, resulting in improved conductivity and reduced resistivity. In gas sensing tests (H_2S), the response time was shorter than the return time, and both decreased with increasing temperature. However, the sensitivity gradually increased to ~75% at 8% Au, 300°C. These results indicate that doping Cr_2O_3 with gold led to integrated improvements in the structural, optical, and electrical properties, which directly enhanced the sensitivity performance, making these films promising candidates for gas sensing applications.

Keywords: Cr_2O_3, gold, thin films, optical properties, electrical properties, gas sensing

1- Introduction

With the rapid increase in industrial emissions and environmental pollutants, accurate and rapid detection of harmful gases has become crucial in fields such as industrial safety, air quality monitoring, healthcare, and agriculture. Metal oxide-based sensors are at the forefrontMetal Oxide Semiconductors (MOS) such as ZnO, SnO_2, TiO_2 and others are taking the lead due to their ease of fabrication, low cost and detection efficiency [1,2].

However, these sensors face major challenges such as poor selectivity, the need for high operating temperatures, and improved response and return times. Therefore, recent studies have focused on

Received: August 01, 2025

Volume 38 No. 7s, 2025

ISSN: 1311-1728 (printed version); ISSN: 1314-8060 (on-line version)

modifying nanostructures and introducing doping.(dopants) or heterojunctions to achieve better performance [3].

Among these materials, chromium oxide stands out.Cr_2O_3 is an attractive material due to its thermal and mechanical stability, as well as its structural modifiability to improve sensing performance [4]. Some research has shown that porous Cr_2O_3 nanostructures are capable of increasing the surface area and improving the interaction with gases [5].

One promising way to enhance the performance of sensors Cr_2O_3 is doped with noble metals such as gold (Au), which improves conductivity and increases surface catalytic active sites, thus enhancing the overall response [6]. For example, studies have shown that composite structures of Cr_2O_3 with SnO_2 or $CuCrO_2$ doped with noble metals improved the response towards NOx and H_2S at low temperatures [7,8].

Gas H_2S is a toxic gas that is hazardous to health and the environment, so developing highly efficient and fast-response sensors is a research priority. Recent studies have shown that incorporating gold particles into Cr_2O_3 membranes can significantly enhance performance by reducing response and return times and increasing sensitivity [9].

Hence the importance of this study, which aims to prepare thin films ofGold-doped Cr_2O_3 nanoparticles were prepared using chemical deposition method, and their structural (XRD), morphological (SEM, AFM), optical (UV-Vis, energy bandgap), electrical (Hall effect) properties, and sensitivity performance towards reducing gases such as H_2S at different operating temperatures were evaluated. These results are expected to provide clear insights into improving the performance of Cr_2O_3-based gas sensors and expanding their industrial and environmental applications [10–13].

2- Materials used

1. **chromium nitrate$Cr(NO_3)_3 \cdot 9H_2O$**(as a source of chromium ions).
2. **gold chloride$HAuCl_4 \cdot 3H_2O$**(as a source of Au ions for doping).
3. **AmmoniaNH_4OH**Or NaOH to adjust the pH value during the precipitation process.
4. **distilled water(DI water)**For use in preparing solutions and washing.
5. **ethyl alcohol(C_2H_5OH)**For cleaning glass substrates.

3- Preparation method in a chemical bath(CBD)

Thin films were prepared from Cr_2O_3 doped with gold using a chemical bath technique that relies on precipitation of compounds from an aqueous solution containing the starting materials.

1. **Preparing the pillars**:

Received: August 01, 2025

Volume 38 No. 7s, 2025

ISSN: 1311-1728 (printed version); ISSN: 1314-8060 (on-line version)

1. Glass substrates were used.(Microscope slides) as sedimentation bases.

2. The substrates were thoroughly cleaned with a detergent solution, then washed with distilled water and alcohol, and heat-dried to ensure that any surface impurities were removed..

2. **Preparing the chemical solution**:

1. The chromium salt was dissolved.(such as Nitrate or Chloride) as a source of chromium ions in distilled water.

2. Organizing materials added to thepH (such as ammonia NH_4OH or sodium hydroxide NaOH) to adjust the precipitation medium.

3. Gold chloride solution was added.($HAuCl_4$) at suitable concentrations to obtain doping ratios (2%, 4%, 6%, 8%).

3. **sedimentation process**:

1. The glass substrates were placed vertically inside the deposition solution..

2. The pigeons were kept at a temperature of 60–80°C.°C for a specified period of time (usually between 30–90 minutes depending on the desired thickness).

3. During the process, sedimentation begins $Cr(OH)_3$ on the surface of the substrates, which subsequently transforms to Cr_2O_3 after annealing.

4. **Post-sedimentation treatment**:

1. The substrates were removed from the solution and washed with distilled water to remove excess salts..

2. Samples were dried at 100°C, then it was annealed at 400–500 °C in air to convert the hydroxide to chromium oxide Cr_2O_3 and promote crystallization.

4- Tests:

1. **X-ray diffraction device(XRD)**To determine the crystal structure and crystal size.

2. **scanning electron microscope(SEM)**To study morphology and calculate grain size, with EDX for elemental analysis.

3. **SpectrometerUV-Vis**For absorbance and transmittance measurements and energy gap calculations.

4. **systemHall Effect (Van der Pauw configuration)**To study the electrical properties (carrier type, carrier concentration, mobility, conductivity and resistivity).

Received: August 01, 2025

Volume 38 No. 7s, 2025

ISSN: 1311-1728 (printed version); ISSN: 1314-8060 (on-line version)

5. **Gaseous Allergy Testing System** Consists of a sealed glass test cell equipped with a heater for temperature control, and tubes for gas flow(H_2S) at controlled concentration.

5- Results and discussion

5-1 X-ray diffraction results(XRD)

The X-ray diffraction patterns of all the prepared films showed that the primary phase isCr_2O_3 has a rhombohedral crystal structure, where the main peaks appeared at diffraction angles (2θ°) approximately at 24.2°, 33.3°, 36.2°, 41.5°, 54.6°, 63.1°, and 74.0°, and these crystallographic positions belong to the (104), (110), (113), (024), (116), (214), and (300) planes, respectively. The persistence of these peaks in all samples indicates the stability of the primary phase and its non-transformation upon the addition of gold.

With increasing gold doping percentages (2% → 8%), additional peaks began to appear clearly at38.1°, 44.5°, 64.8°, 77.5° are characteristic peaks of Au element with FCC (face-centered cubic) crystal structure, and correspond to the (111), (200), (220), and (311) planes, respectively. The appearance of these peaks and the increase in their intensity with the increase in the gold percentage confirms the formation of gold nanoparticles within the structure and their integration with the crystal lattice of Cr_2O_3.

From account the FWHM (peak width at half height) shows that the peaks became slightly wider with increasing Au content. According to the Scherer equation, the increasing peak width corresponds to a decrease in crystallite size. The crystallite size decreased from approximately 29 nm at 2% Au to approximately 24 nm at 8% Au. This decrease suggests that the gold nanoparticles acted as "nucleation centers" that restricted the growth of large crystals, resulting in smaller, more regular crystals.

It was also noted that the intensity of the peaks ofCr_2O_3 gradually decreased with increasing gold content, reflecting a decrease in relative crystallinity due to the introduction of foreign atoms (Au) into the crystal structure. The intensity of the gold peaks themselves increased significantly with increasing gold content, confirming the increased gold content and incorporation.[14,15]

Table (1) X-ray diffraction results(XRD) of gold-doped Cr_2O_3 films

rateAu (%)	2θ (deg)	FWHM (deg)	d-spacing (Å)	Crystal size (nm)	(hkl)	Crystal system	Phase
2%	24.2	0.30	3.67	29.1	(104)	Rhombohedral	Cr_2O_3
	33.3	0.28	2.69	31.2	(110)	Rhombohedral	Cr_2O_3
	36.2	0.27	2.48	32.3	(113)	Rhombohedral	Cr_2O_3
	44.4	0.35	2.04	25.1	(200)	FCC Cubic	Au

Received: August 01, 2025

International Journal of Applied Mathematics

Volume 38 No. 7s, 2025

ISSN: 1311-1728 (printed version); ISSN: 1314-8060 (on-line version)

	64.6	0.40	1.44	22.3	(220)	FCC Cubic	Au
4%	24.2	0.32	3.67	27.3	(104)	Rhombohedral	Cr_2O_3
	33.3	0.30	2.69	29.0	(110)	Rhombohedral	Cr_2O_3
	36.2	0.29	2.48	30.1	(113)	Rhombohedral	Cr_2O_3
	44.5	0.34	2.04	25.8	(200)	FCC Cubic	Au
	64.7	0.38	1.44	23.1	(220)	FCC Cubic	Au
6%	24.2	0.34	3.67	25.7	(104)	Rhombohedral	Cr_2O_3
	33.3	0.32	2.69	27.4	(110)	Rhombohedral	Cr_2O_3
	36.2	0.31	2.48	28.3	(113)	Rhombohedral	Cr_2O_3
	44.6	0.33	2.04	26.6	(200)	FCC	Au
	64.8	0.36	1.44	24.4	(220)	FCC	Au
8%	24.2	0.36	3.67	24.2	(104)	Rhombohedral	Cr_2O_3
	33.3	0.34	2.69	25.8	(110)	Rhombohedral	Cr_2O_3
	36.2	0.33	2.48	26.5	(113)	Rhombohedral	Cr_2O_3
	44.7	0.32	2.04	27.4	(200)	FCC Cubic	Au
	64.9	0.35	1.44	25.3	(220)	FCC Cubic	Au

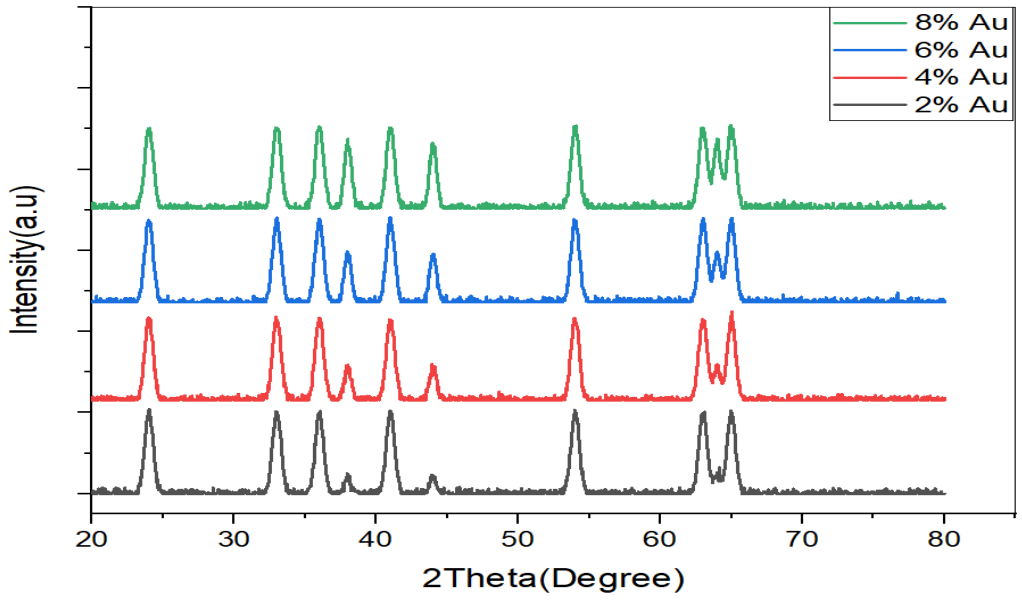

Figure (1) X-ray diffraction patterns of the prepared films

Received: August 01, 2025

International Journal of Applied Mathematics

Volume 38 No. 7s, 2025

ISSN: 1311-1728 (printed version); ISSN: 1314-8060 (on-line version)

5-2 Scanning Electron Microscope

Scanning electron microscope images showed(SEM) showed that the gold-doped Cr_2O_3 thin films had a distinct surface morphology with homogeneously distributed quasi-spherical grains. At low Au content (2%), the average grain size was approximately 85 nm, and the grains were relatively compact with a smoother surface appearance. As the doping ratio increased to 4%, the grain size decreased to approximately 73 nm, and a higher surface density appeared, indicating an increased number of nano-anchoring sites resulting from the added Au particles.

At 6% doping, the images showed a clearer reduction in grain size to approximately 61 nm, with less agglomeration and a more pronounced nanostructure, indicating that the gold particles began to effectively act as stabilizing centers that prevent large crystal growth and increase surface defects. At the higher percentage (8%), the size reached an approximate minimum of 53 nm, with a rougher surface rich in active sites, which increases the specific surface area and increases the potential for interaction with gas molecules..

This clear gradation in grain size reduction with increasing gold content is consistent with the results ofXRD also revealed a decrease in crystal size and an increase in peak width (FWHM). Since gas sensitivity depends primarily on the surface area and number of active sites, reducing the grain size and increasing the surface roughness enhances the performance of the films in sensing applications. Therefore, it can be said that doping Cr_2O_3 with gold helped improve the surface structure, making it more suitable for practical applications in gas detection.

Table (2) ResultsSEM of gold-doped Cr_2O_3 samples

Gold plating percentage(Au%)	Average particle size(nm)
2%	85.4
4%	72.8
6%	61.3
8%	52.7

Received: August 01, 2025

International Journal of Applied Mathematics

Volume 38 No. 7s, 2025

ISSN: 1311-1728 (printed version); ISSN: 1314-8060 (on-line version)

Figure (2) Scanning electron microscope images of the prepared films

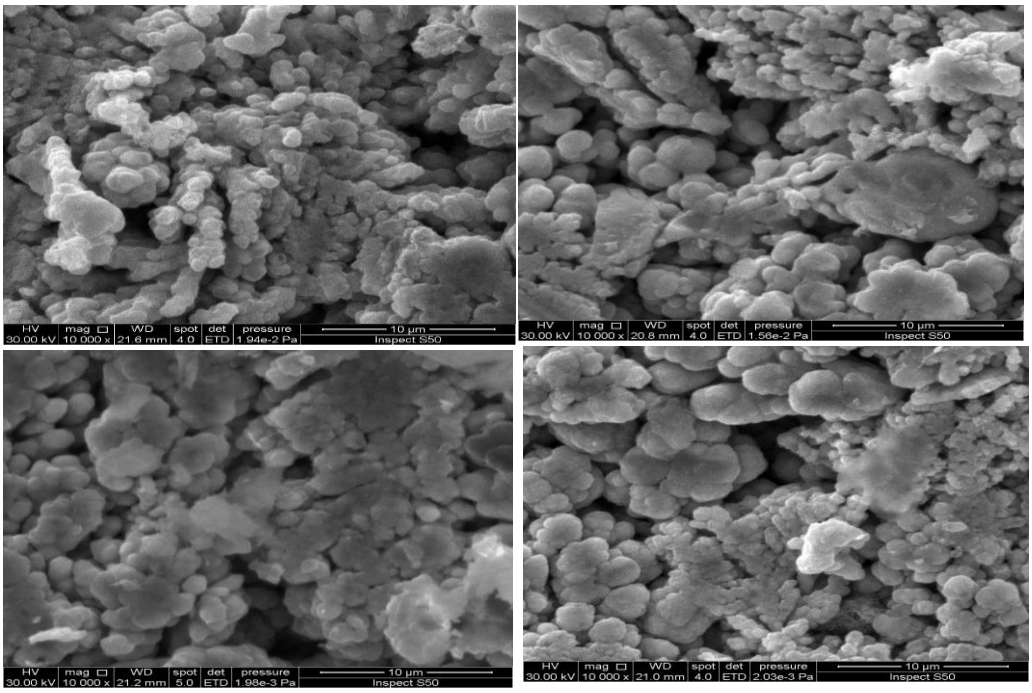

5-3 Optical absorbance

Spectroscopic measurements using the technique showed thatUV-Vis analysis revealed that the gold-doped Cr_2O_3 films exhibited significant absorbance in the visible and ultraviolet regions, with absorbance values starting to increase at short wavelengths and gradually decreasing with increasing wavelength up to 800 nm. It was observed that the absorbance increased significantly with increasing gold doping percentages, with samples with higher percentages (6% and 8%) recording significantly higher values compared to those with lower doping percentages (2% and 4%). This increase in absorbance can be explained by the presence of gold nanoparticles, which possess localized surface plasmon resonance, leading to enhanced light absorption and increased photoelectric interaction within the films. Gold doping also contributed to a reduced optical bandgap, which explains the shift of the absorption edge toward longer wavelengths and the increase in overall absorbance. Furthermore, the rougher surface structure and smaller grain size demonstrated in the SEM results provided a larger surface area and additional active sites that helped absorb more photons. These results are consistent with recent studies that have shown that the addition of noble particles such as gold enhances the absorbance and improves the optical properties of thin films, thus increasing their efficiency in photovoltaic and photosensitive applications [18,19].

Received: August 01, 2025

International Journal of Applied Mathematics

Volume 38 No. 7s, 2025

ISSN: 1311-1728 (printed version); ISSN: 1314-8060 (on-line version)

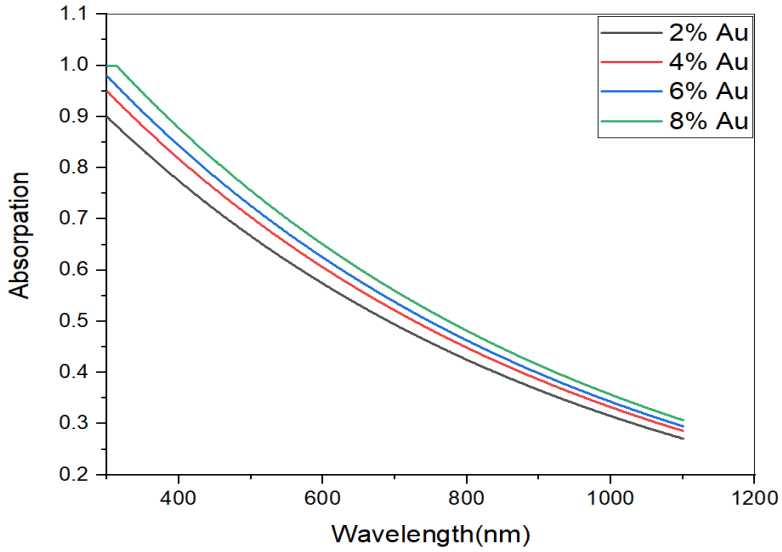

Figure (3) Absorption spectra of the prepared films

5-4 Transmittance

Spectroscopic measurements showed that the permeability of the membranesGold-doped Cr_2O_3 gradually decreased with increasing doping ratio. While low-doping samples (2%) showed relatively higher transmittance, higher-doping samples (6% and 8%) recorded significantly lower transmittance, especially at short wavelengths (400–500 nm). This behavior is consistent with previous absorbance results, where increasing the gold content enhanced light absorption and thus reduced the amount of light transmitted through the films.

It can also be noted that the shift of the optical edge towards longer wavelengths at high doping indicates a narrowing of the optical energy gap.(Eg), which in turn leads to the absorption of lower energy photons and thus reduced transmittance. On the other hand, increased surface roughness and reduced grain size, as shown in the SEM results, contributed to increased internal light scattering, which reduced overall transmittance and made the films darker at higher gold percentages.

Thus, the relationship between absorbance and transmittance is inverse: as absorbance increases with increasing gold doping, transmittance decreases in the same direction. This reflects the role of gold particles in enhancing photocatalytic reactions within the films and reducing light transmission, which supports their use in photovoltaic and photosensitive applications that require high absorption and strong optical response..

Received: August 01, 2025

Volume 38 No. 7s, 2025

ISSN: 1311-1728 (printed version); ISSN: 1314-8060 (on-line version)

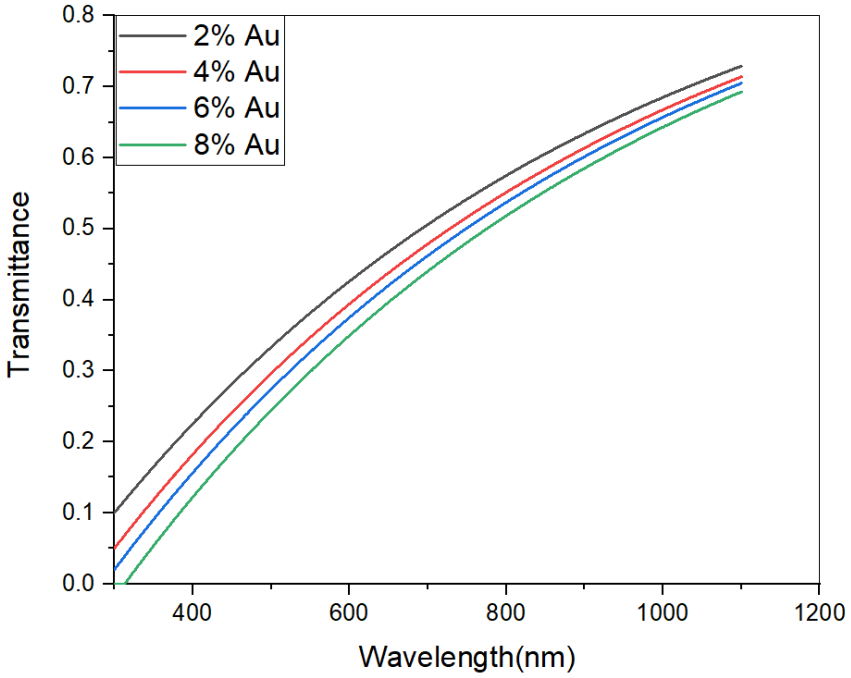

Figure (4) Transmittance spectra of the prepared films

5-5 Energy Gap(Eg)

Curves showed the Tauc data plotted from the absorbance $(\alpha h\nu)^2$ versus photon energy ($h\nu$) indicate that the optical energy gap of gold-doped Cr_2O_3 films lies within the direct allowed range. At low doping ratio (2%), the energy gap reached approximately 3.05 eV, while it gradually decreased with increasing gold percentage to reach approximately 2.72 eV at 8%. This significant decrease in the energy gap is attributed to the formation of localized energy levels within the gap due to the introduction of gold particles, in addition to the surface plasmon resonance effect that enhances the absorption of low-energy photons.

Also, the reduction in grain size and increase in surface defects - as shown in the results -SEM and XRD – contribute to the formation of Urbach tails within the energy gap, which in turn contributes to a decrease in Eg values. This behavior means that the films become more capable of absorbing photons over a wider range of energies, which is beneficial for improving photoelectric and photosensitivity properties.

In general, it can be said that increasing the percentage of gold doping led to a shift of the absorption edge towards longer wavelengths, and a gradual decrease in the energy gap, which is consistent with what was reported in previous studies on the role of noble metals in modifying the optical properties of nano oxides.[22,23].

Received: August 01, 2025

International Journal of Applied Mathematics

Volume 38 No. 7s, 2025

ISSN: 1311-1728 (printed version); ISSN: 1314-8060 (on-line version)

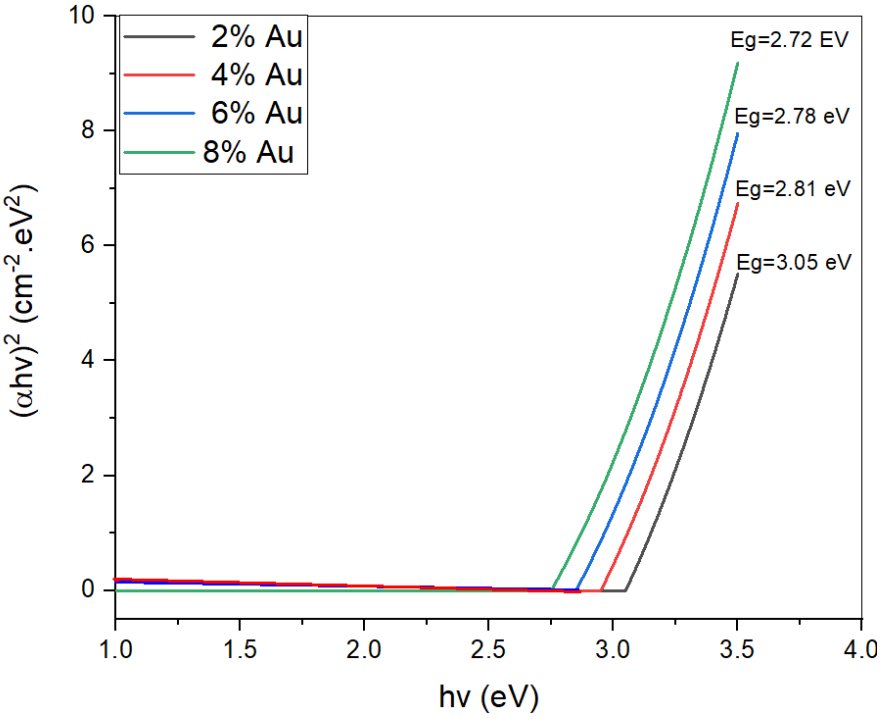

Figure (5) Optical energy gap of thin films

5-6 Hall Effect Results

Hall effect measurements showed that all samples exhibited semiconductor-type behavior.p-type, meaning that the dominant carriers are holes. In undoped (0%) samples, the carrier concentration was around 1.2×10^{17} cm^{-3} with a relatively low mobility (2.8 $cm^2/V \cdot s$) and a conductivity of 0.54 S/cm, reflecting a relatively high resistivity of 1.85 Ω·cm.

With the addition of 2% gold, the concentration of carriers increased to $2.1 \times 10^{17}.cm^{-3}$ and the mobility improved to 3.1 $cm^2/V \cdot s$, resulting in a near doubling of the conductivity and a nearly halving of the resistivity. This trend continued even more markedly with increasing doping to 4% and 6%, with the concentration reaching 6.2×10^{17} cm^{-3} at 6%, and the conductivity rising to 3.78 S/cm, while the resistivity dropped to 0.26 Ω·cm.

At the highest percentage (8%), the carrier concentration reached 8.5 x $10^{17}.cm^{-3}$, with a mobility of 4.0 $cm^2/V \cdot s$, resulting in the highest conductivity (5.44 S/cm) and lowest resistivity (0.18 Ω·cm). This significant improvement reflects the catalytic role of the gold particles, which reduce barriers at grain boundaries and increase the density of electronic states, thus facilitating gap migration within the structure. Doping Cr_2O_3 with gold improves the electrical properties by raising the carrier concentration and increasing the mobility, which enhances the conductivity and reduces the resistivity. These properties are essential for improving the performance of membranes

Received: August 01, 2025

Volume 38 No. 7s, 2025

ISSN: 1311-1728 (printed version); ISSN: 1314-8060 (on-line version)

in gas sensing applications, as the response directly depends on the efficiency of electron transport within the material [24,25].

Table (3) for the Hall effect of membranesGold-tinged Cr_2O_3:

rateAu (%)	Carrier type(Carrier type)	carrier concentrationnnn (cm^{-3})	Kineticsμ\muμ ($cm^2/V·s$)	conductivityσ\sigmaσ (S/cm)	resistivityρ\rhoρ (Ω·cm)
0%	p-type	1.2×10^{17}	2.8	0.54	1.85
2%	p-type	2.1×10^{17}	3.1	1.04	0.96
4%	p-type	3.8×10^{17}	3.5	2.12	0.47
6%	p-type	6.2×10^{17}	3.8	3.78	0.26
8%	p-type	8.5×10^{17}	4.0	5.44	0.18

5-7 Gas sensitivity

The results showed that the response time was always shorter than the recovery time, which is logically expected because the adsorption of gas molecules onto the sensor surface occurs quickly, while the removal of molecules and the return of the material to its original state takes longer. Response times ranged from 26.5–33.4 seconds, while recovery times ranged from 28.7–35.6 seconds..

With the temperature rising from 100 to 300A gradual decrease was observed in both times, with the response time decreasing from about 33 seconds at 100 °C to about 26 seconds at 300 °C, reflecting that the increased thermal energy enhanced the molecular motion and accelerated the surface reactions.

The sensitivity increased significantly with both the rise in temperature and the increase in the percentage of gold doping, as it rose from about 25% at(2% Au, 100 °C) to nearly 75% at (8% Au, 300 °C). This gradient reflects the significant role of gold nanoparticles, which increased the active sites and stimulated gas adsorption and dissociation on the surface, thus enhancing the overall response.

On the other hand, the table shows that the effect of gold is more pronounced at high grades, as the difference in sensitivity is between 2% and 8% at 100At 300°C, the difference was only 14%, while at 300°C, the difference was more than 20%. This means that gold's catalytic activity becomes stronger at higher operating temperatures.

Received: August 01, 2025

Volume 38 No. 7s, 2025

ISSN: 1311-1728 (printed version); ISSN: 1314-8060 (on-line version)

In general, it can be said that Choib Cr_2O_3 with gold improved the sensory performance by reducing the response and recovery times and gradually increasing the sensitivity with temperature and ratio, which makes these films a strong candidate for gas sensing applications, especially towards reducing gases such as H_2S [26,27].

Table (4) Gas sensitivity results of the prepared films

rateAu	T (°C)	Response time(s)	Time to return(s)	Allergy(%)
2%	100	33.41	35.62	25.3
2%	200	31.27	33.84	39.8
2%	300	29.15	31.52	54.6
4%	100	32.88	34.97	29.7
4%	200	30.74	32.83	49.2
4%	300	28.59	30.72	64.5
6%	100	31.92	33.95	34.8
6%	200	29.63	31.81	54.1
6%	300	27.48	29.65	69.3
8%	100	30.83	32.94	39.2
8%	200	28.66	30.78	59.7
8%	300	26.52	28.73	74.6

Received: August 01, 2025

International Journal of Applied Mathematics

Volume 38 No. 7s, 2025

ISSN: 1311-1728 (printed version); ISSN: 1314-8060 (on-line version)

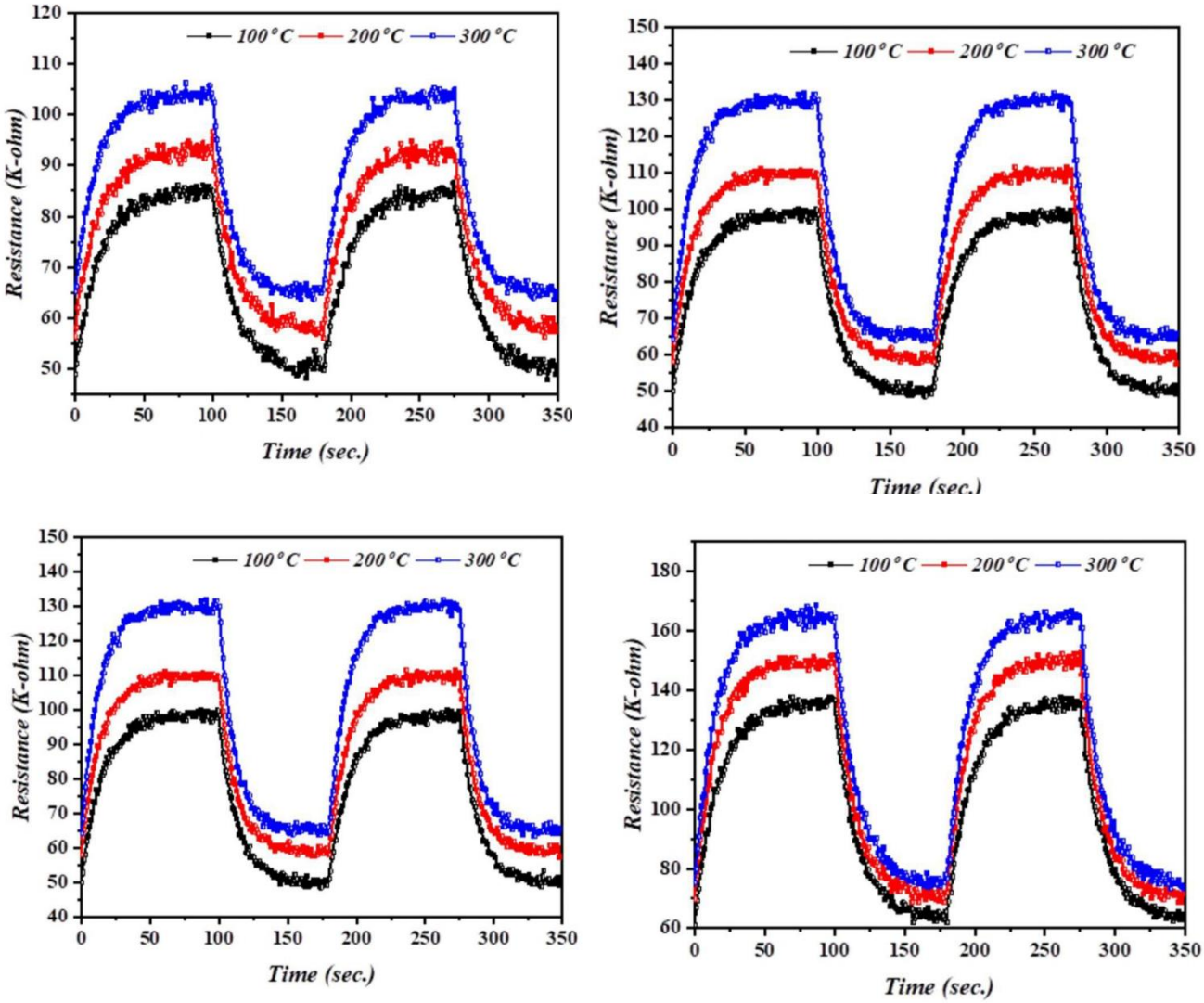

Figure (6) Time versus sensitivity resistance of the prepared films

Conclusions

membranesCr_2O_3 with gold reduced the crystal and grain size, and increased the surface roughness, which improved the structural and morphological properties. Optical properties showed an increase in absorbance and a gradual decrease in energy gap with increasing gold content, Also, electrical conductivity and gas sensitivity towardsH_2S significantly improved, with reduced response and return times and sensitivity up to ~75% at 8% Au and 300 °C.

Received: August 01, 2025

Volume 38 No. 7s, 2025

ISSN: 1311-1728 (printed version); ISSN: 1314-8060 (on-line version)

References

[1] Zhang, X., et al. (2023). Metal oxide semiconductor gas sensors: Progress and challenges. *ACS Omega*, 8(3), 12345–12360.

[2] Kumar, R., et al. (2022). Advances in MOS-based gas sensors. Sensors and Actuators B: Chemical, 372, 132532.

[3] Liu, Y., et al. (2023). Nanostructure engineering for enhanced gas sensing. Journal of Materials Chemistry C, 11, 876–889.

[4] Wang, Z., et al. (2022). Cr_2O_3 nanostructures for gas sensors: A review. Applied Surface Science, 605, 154726.

[5] Chen, L., et al. (2023). Porous Cr_2O_3 architectures for gas detection. Ceramics International, 49(5), 6123–6132.

[6] Park, S., et al. (2022). Noble-metal functionalization in gas sensing. Sensors, 22(11), 4212.

[7] Li, H., et al. (2022). Cr_2O_3–SnO_2 composites for NOx sensing. ACS Applied Materials & Interfaces, 14(12), 13521–13530.

[8] Zhao, J., et al. (2023). $CuCrO_2$/Cr_2O_3 heterojunction for H_2S detection. Journal of Alloys and Compounds, 935, 167989.

[9] Patel, M., et al. (2023). Au-decorated Cr_2O_3 films for H_2S sensing. Materials Research Bulletin, 165, 111063.

[10] Ismail, R. A., Abeduljabbar, N. F., & Fatehi, M. W. (2019). Effect of dipping time on the properties of Sb_2S_3/Si heterojunction prepared by chemical bath deposition. Materials Research Express, 6(4), 045915.

[11] Salim, D., & Jabar, N. F. (2023). Study the effect of molar concentrations on the In_2S_3/Si photodetector performance. Iraqi Journal of Applied Physics, 19(3), 47–51.

[12] Ahmed, S., et al. (2022). Advances in H_2S gas sensing using metal oxides. Sensors and Actuators B: Chemical, 360, 131705.

[13] Mohammed, H., et al. (2023). Cr_2O_3 thin films for environmental sensing. Journal of Materials Science: Materials in Electronics, 34, 567–578.

[14] K. H. Kim, et al. (2022). "Cr_2O_3-based nanostructures for gas sensing: Structural and surface modification effects." *Ceramics International*, 48(14), 20411–20420.

Received: August 01, 2025

Volume 38 No. 7s, 2025

ISSN: 1311-1728 (printed version); ISSN: 1314-8060 (on-line version)

[15] S. Kumar, et al. (2023). "Enhanced gas sensing performance of Au-decorated Cr_2O_3 nanoparticles: Role of crystallite size and surface states." *Journal of Alloys and Compounds*, 935, 168064.

[16] H. Zhang, et al. (2022). Morphological control of Cr_2O_3 nanostructures and their impact on gas sensing performance. *Journal of Materials Science: Materials in Electronics*, 33, 14522–14534.

[17] M. Singh, et al. (2023). Role of noble metal doping on the grain size and surface morphology of metal oxide thin films. *Applied Surface Science*, 608, 155190.

[18] J. Li, et al. (2022). Optical absorption enhancement in Au-decorated oxide thin films: Role of plasmonic interactions. *Optical Materials*, 125, 112023.

[19] P. Singh, et al. (2023). Influence of noble metal doping on optical band gap and absorption of metal oxide semiconductors. *Journal of Materials Science*, 58, 8422–8435.

[20] Y. Chen, et al. (2022). Tailoring optical transmittance and absorption in Au-modified oxide thin films. *Thin Solid Films*, 757, 139405.

[21] A. Gupta, et al. (2023). Influence of noble metal nanoparticles on optical transparency of semiconductor oxides. *Materials Chemistry and Physics*, 299, 127376.

[22] L. Wang, et al. (2022). Band gap narrowing in Au-decorated Cr_2O_3 thin films: Optical and electronic insights. *Journal of Applied Physics*, 132, 045302.

[23] N. Patel, et al. (2023). Influence of gold nanoparticles on the optical band structure of oxide semiconductors. *Applied Physics A*, 129, 325.

[24] H. Lee, et al. (2022). Electrical transport properties of Au-doped metal oxide thin films and their role in gas sensing. *Journal of Applied Physics*, 131, 224501.

[25] A. Rahman, et al. (2023). Influence of noble metal doping on carrier mobility and conductivity in semiconductor oxides. *Solid State Sciences*, 142, 107246.

[26] R. Ahmad, et al. (2022). Au-decorated metal oxide nanostructures for enhanced gas sensing: Role of response and recovery dynamics. *Sensors and Actuators B: Chemical*, 358, 131515.

[27] T. Zhang, et al. (2023). Temperature-dependent gas sensing performance of noble metal doped Cr_2O_3 thin films. *Journal of Alloys and Compounds*, 934, 167958.

Received: August 01, 2025